Challenges with Harmonic Compensation at a Remote Bus in Offshore Wind Power Plant

Sanjay K. Chaudhary, Cristian Lascu, Bakhtyar Hoseinzadeh, and Remus Teodorescu
Department of Energy Technology
Aalborg University
Aalborg, Denmark

Łukasz H. Kocewiak, and Troels Sørensen
DONG Energy Wind Power
Fredericia, Denmark

Christian F. Jensen
Energinet.dk
Fredericia, Denmark

***Abstract*—This paper investigates the challenges associated with remote harmonic compensation in offshore wind power plants through long cables and transformers. The interaction between the grid network and the wind power plant network can lead to the amplification of certain harmonics and potentially resonant conditions. Hence, the plant developer is required to maintain the harmonic distortion at the point of common coupling within the planning level limits using harmonic compensation, which is usually done by static filters. In this paper an active damping compensation strategy with a STATCOM using emulation of resistance at the harmonic frequencies of concern is analyzed. Finally the results are demonstrated using time domain simulations in PSCAD.**

Keywords—harmonic distortion, active power filter, resonance, damping, wind power plants.

I. Introduction

Offshore wind power plants (WPPs) are connected to the onshore grid using long high voltage cables, and usually a transformer at the grid end. Besides there is a large amount of cables in the collector grid. The combination of the transformer reactance and the cable capacitances can lead to the amplification of harmonic distortion levels and potential resonances [1]. There are harmonic standards like IEEE [1] and IEC [2] which define the harmonic limits and standards. Engineering Recommendation G5/4-1 [3] defines the planning levels for the grid connection of the non-linear equipment.

Power electronic converters and non-linear loads are the main sources of harmonics in the grid. The background harmonic data indicates the effect of all such sources at a specified terminal. When the wind power plant (WPP) is connected to such a network, it tends to change the effective grid impedance at the point of connection (POC). Depending upon the interaction between the grid impedance and the impedance posed by the WPP, the background harmonic levels may get amplified or attenuated at the POC.

Harmonic sources are invariably present in the power system network, and hence there is some amount of harmonic distortion even before the WPP is connected. The grid connection of the WPP might lead to the amplification or attenuation of the harmonic distortions depending upon interaction between the equivalent grid impedance and the impedance presented by the WPP. Such an amplification of harmonic distortion at the POC might lead to unacceptable levels of harmonic distortion and poor power quality. Moreover, the power converters present in the WPP, might also be injecting certain amount of harmonics in the power system.

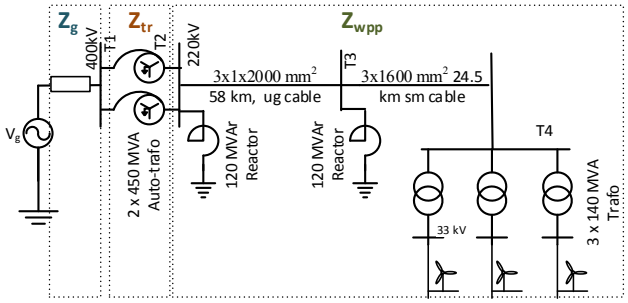

Fig. 1. WPP electrical network model.

This paper describes the harmonic distortions due to the background grid harmonic sources hand the impedance interactions between the grid and the WPP impedances. Harmonic current injection from the wind turbines (WTs) in the WPP is ignored here. Afterwards, active damping of the harmonic distortions is provided by a STATCOM which emulates resistive behavior at the concerned frequencies. It is demonstrated that the compensation works for the local bus where the harmonic filtering action is provided, while it is not effective at other buses, referred to as the remote bus in this paper. Incidentally, the POC and the point of common coupling (PCC) are usually at the high voltage buses and hence not preferred buses for the connection of a STACOM or an active filter. However, the harmonic compliance is measured at such remote buses. This paper evaluates the challenges of harmonic filtering on such remote buses.

II. Test WPP Grid System

A. Wind power plant model

The 400 MW Anholt offshore WPP has been used as a reference for developing the test WPP network as shown in Fig 1 [5]. There are 3x140 MVA, 225/32 kV plant step up transformers to connect the collector bus to the 220 kV export cables, which consist of 24.5-km submarine cable and 58-km underground cables. Finally it is connected to the onshore grid using two 450 MVA, 410/233 kV transformers. Shunt reactors are provided for the compensation of cable capacitance.

This work is supported by Energinet.dk through the project "Active filter functionalities for power converters in wind power plants" (Forskel program, PSO-2014-1-12188).

978-1-5090-2320-2/16/$31.00 ©2016 IEEE

TABLE I. BASE VALUES.

	Grid and T1	T2, T4, and HV cables
Power [MW]	400	400
RMS Voltage [kV]	400	220
RMS Current [A]	577.4	1049.7
Resistance [Ω]	400	121

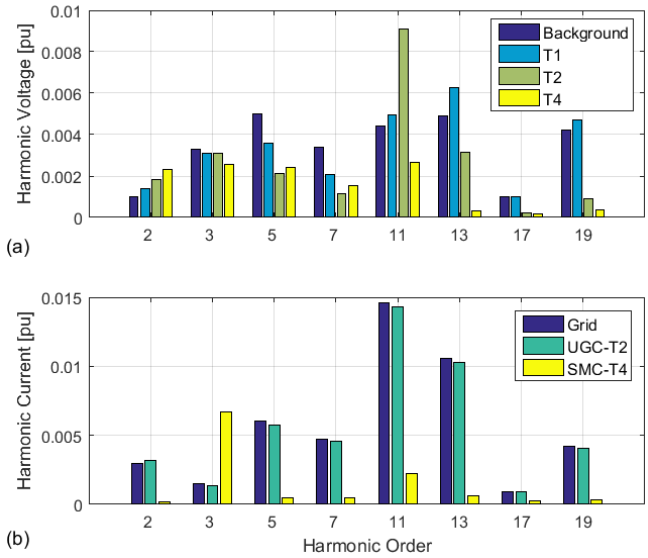

Fig. 2. Base case. (a) Background harmonic levels, and the harmonic voltages at T1, T2 and T4, and (b) Harmonic current flow in the grid and the HV cables at T1, T2 and T4.

Although the collector grid comprises different types and lengths of medium voltage (MV) cables, it is represented here by 3x4x11-km long network of MV cables at 34 kV.

B. Grid

The onshore grid is represented by a Thevenin equivalent voltage source which includes the three phase fundamental voltage at the nominal level along with the different harmonic components. The magnitudes of the background harmonic voltages at the selected orders are shown in Fig. 2. It also shows the resultant harmonic voltages observed at the PCC bus T1 and other buses T2 and T4 in the WPP grid along with the harmonic current flowing in the grid and the high voltage (HV) cables. The base values of the voltage and currents for the computation of the per unit (pu) values are defined on the basis of 400 MW as the base power and the nominal bus voltages as the base voltage at different buses and is given in Table I.

The frequency dependent grid impedance is first obtained in tabular form as impedance versus frequency characteristics. For frequency domain analyses like the frequency scan or the harmonic power flow, it can be directly used. However, for time domain simulation studies, the data has to be converted into a transfer function for the frequency dependent network equivalent (FDNE) using vector fitting algorithm [4]. The impedance versus frequency characteristics of the actual grid impedance data and the fitted FDNE transfer function is shown in Fig. 3.

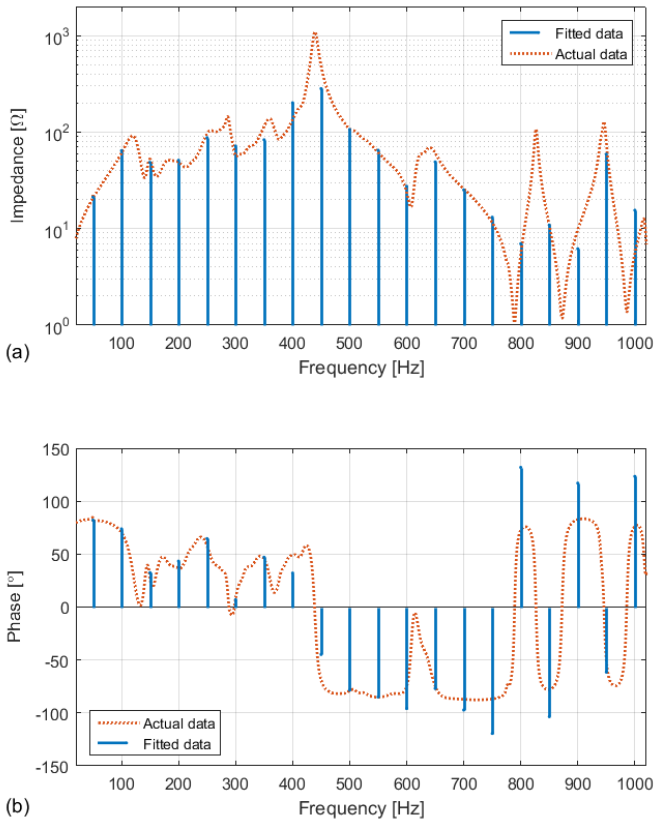

Fig. 3. Grid impedance characteristics. (a) Magnitude, and (b) Phase angle.

C. Amplification/Attenuation of harmonic distortion

The interaction between the grid impedance, which is the Thevenin equivalent impedance of the onshore grid, in series with the impedances of the grid connection system, and the WPP impedance, which is the combined impedance of the cable systems and WTGs, leads to the amplification/attenuation of the harmonic distortion at different buses in the system. In this work, the 400 kV bus T1 is considered as the PCC, and hence the harmonic distortion at bus T1 should be checked within applicable limits.

Assuming that the grid is the main source of harmonic distortion, and the WTs are switched off and they do not inject any harmonics in this study, the amplification or attenuation of the harmonic distortion at buses T1 and T2 in the test system is given by,

$$\left.\begin{aligned} A_1 &= \frac{V_{1h}}{V_h} = \frac{Z_{tr,h} + Z_{wpp,h}}{Z_{g,h} + Z_{tr,h} + Z_{wpp,h}} \\ A_2 &= \frac{V_{2h}}{V_h} = \frac{Z_{wpp,h}}{Z_{g,h} + Z_{tr,h} + Z_{wpp,h}} \end{aligned}\right\} \quad (1)$$

where, the $Z_{tr,h}$, $Z_{wpp,h}$ and $Z_{g,h}$ are the total impedance of the transformer, the WPP and the grid observed at the *h*-th harmonic order as shown in the equivalent single line diagram in Fig. 4. The two amplification ratios at different frequencies are plotted in Fig. 5. A value greater than unity indicates amplification and lower than unity indicates attenuation. Amplification is observed for the harmonic orders 2nd, 9-15th, 17th and the 19th harmonic

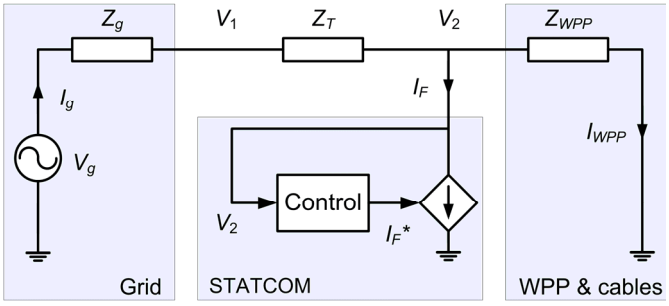

Fig. 4. An equivalent single line drawing of the test system.

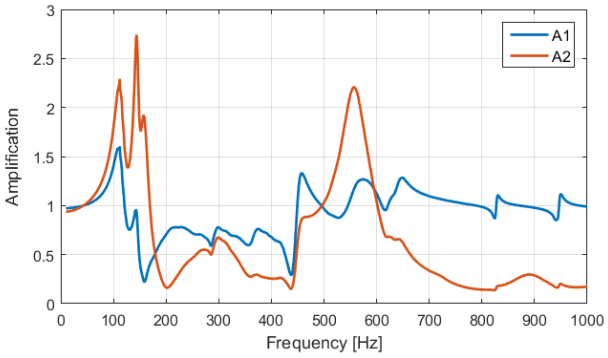

Fig. 5. Amplification of the background harmonics in the grid.

orders at bus T1. Similarly, the 2nd, 11th and the 12th harmonics get amplified at bus T2.

The amplification of 1.27 at the 13th harmonic can be explained by the positive sequence impedance values of, $Z_{g,13} = (17 - j59)\Omega$ and $\left(Z_{tr,13} + Z_{wpp,13}\right) = (48 + j233)\Omega$ referred to the base of 400kV. Typically, the odd harmonics at the 5th, 7th, 11th, 13th, 17th and 19th have a relatively higher content in the background harmonics in the grid.

D. STATCOM controller for harmonic compensation

Connecting a resistor for harmonic compensation is not feasible due to high losses. It is therefore emulated by a STACOM, which provides reactive power compensation at the fundamental frequency and selective harmonic filtering. Fig. 6 shows the block diagram of the STATCOM controller for the active power filter (APF) functionality to provide the harmonic compensation. It will be in addition to the reactive power regulation, which happens at the fundamental frequency, and that is beyond the scope of this paper.

The controller needs to extract the components of bus voltage at the desired harmonic orders. The Park's transformation yields the *dq* components with dc values for the particular harmonic order used in the transformation, and ac components due to the fundamental and other harmonic components in the input voltage. Such ac components are filtered out using a second order filter with coincident real poles at −2 rad/sec. The remaining dc components are inverted into the phase domain.

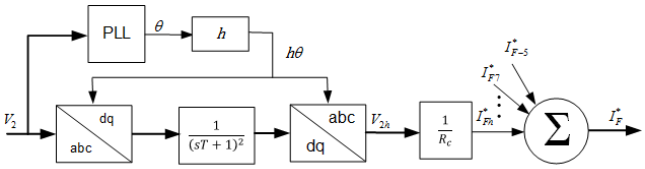

Fig. 6. STATCOM controller for harmonic compensation.

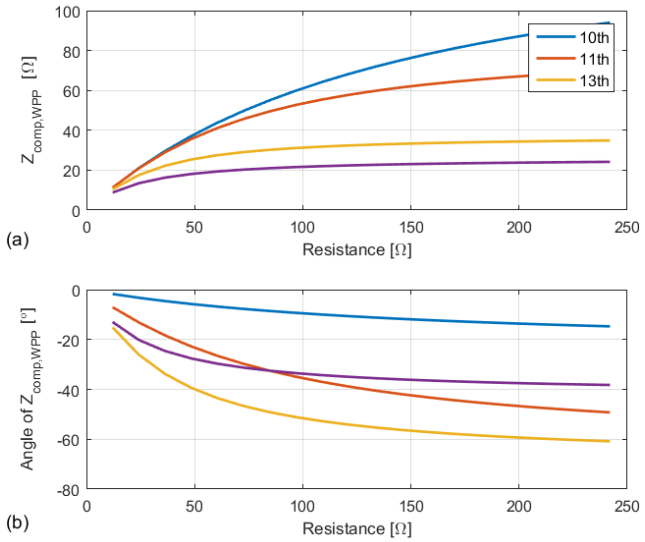

Fig. 7. Variation of WPP impedance with resistance connected at T2. (a) Magnitude. (b) Phase.

The harmonic voltages are then divided by the desired value of the harmonic resistance, R_c, to obtain the corresponding harmonic current reference. In this way the current references are obtained for the desired harmonic orders, and then they can be added together in phase domain. The compensating resistance could be the same or they may differ for different harmonic components. Thus, the current references are proportional to the corresponding harmonic voltages.

III. Harmonic Compensation Analysis

The WPP network is largely a radial network. When a compensating resistor is connected at a bus, the equivalent impedance of the network, downstream from that bus, decreases. Thus the system impedance characteristic gets changed. Consequently, the harmonic voltages at different buses in the system would change. The resultant amplification ratios for different cases with two different values of the harmonic filtering resistance connected at two different buses are numerically analyzed using (1).

A. Active damping using harmonic resistance at bus T2

When a resistance is connected at T2, it is in parallel to the WPP impedance. Hence, the effective WPP impedance is lower in magnitude and its phase angle moves closer to 0°, implying that it is more resistive as shown in Fig. 7. However, if the WPP, $Z_{comp,wpp}$, impedance is resistive in the uncompensated case, the

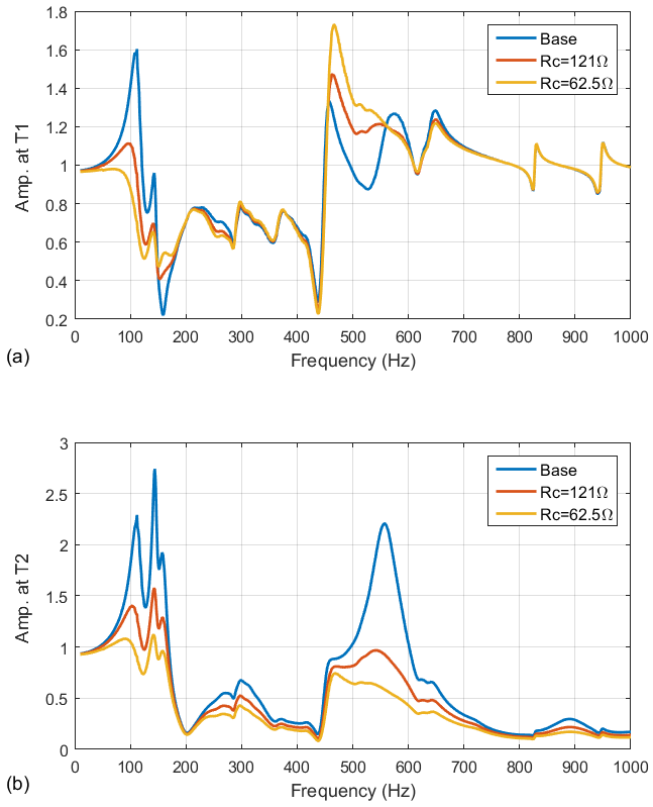

Fig. 8. Amplification due to compensation at T2.

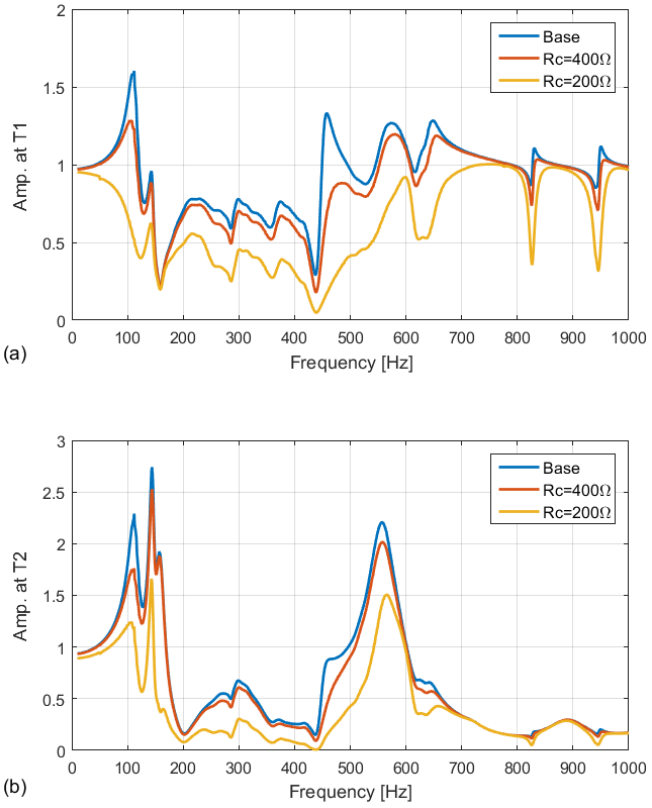

Fig. 9. Amplification due to compensation at T1.

TABLE II. 10TH HARMONIC IMPEDANCE OBSERVED AT T1.

	Real	Imaginary
Z_g [Ω]	20	-108
$Z_{wpp}+Z_{tr}$ [Ω]	424	77
$Z_{comp,wpp}+Z_{tr}$ [Ω]	138	245

the resultant resistance may be smaller than the value in the uncompensated case.

Physically, the resistors in harmonic power filters dissipate energy, and thus provide damping to harmonic amplifications. Likewise, the APF can provide damping to harmonic amplifications by emulating resistive behavior at the selected harmonic frequencies [6]. This is the case for providing harmonic compensation at the local bus.

For the frequency domain analysis, a shunt resistor is connected at bus T2, in parallel to the WPP impedance, Z_{wpp}, and hence the effective impedance of the parallel combination is lower than that of WPP alone. Therefore, the resultant impedance has a smaller magnitude and its phase angle is closer to 0°. The resultant amplifications at bus T1 and bus T2 are shown in Fig. 8. These curves show that while the compensation works for the full range of harmonics at bus T2, it is not effective at the remote bus T1 as the 6th, 7th, 10th, and 11th harmonic voltages get amplified.

As shown in Fig. 8, the harmonic compensation, provided by the resistances of sizes 1 pu (121 Ω) and 0.5 pu (62.5 Ω) respectively at bus T2, reduces the local amplification ratio. However, it is not the same for the remote bus, T1, which is upstream. An amplification is observed here, in the base case, as the grid impedance is capacitive while the WPP side impedance is inductive. Even though there is an attenuation of the 10th harmonic at the local bus T2, this harmonic gets amplified in comparison to the base case at T1. This can be attributed to the reduced damping due to the reduction of the effective resistance of the WPP from 424 Ω to 138 Ω due to the compensation as shown in Table II.

B. *Active damping using harmonic resistance at bus T1*

As shown in Fig. 9, when the harmonic compensating resistances of sizes 1 pu (i.e. 400 Ω) and 0.5 pu (i.e. 200 Ω) respectively are connected at bus T1, the harmonic voltage gets reduced for the local bus T1 as well as bus T2, which lies downstream. It is expected, as the harmonic voltages are appearing due to background harmonics in the grid.

IV. SIMULATION RESULTS

Harmonic powerflow analysis [7] is used to compare the harmonic level of bus voltages and currents through different components in the system. Afterwards, the performance of dynamic harmonic compensation is shown using time domain simulation in PSCAD.

A. *Harmonic powerflow analysis*

One pu resistance is separately connected to bus T1 and T2. The resultant harmonic voltages at buses T1, T2 and T4 are observed in the test system. The results are compared in Fig. 10.

In line with the amplification ratios described in the previous section, the compensation at bus T1 leads to a reduction of voltage harmonics at all the aforementioned buses. The compensation at bus T2 leads to the reduction of harmonics at bus T2 and T4, which are downstream, while there is an amplification of the 7th and the 11th harmonic at bus T1. The results corroborate the prediction made in the previous section as the distortion levels at bus T2 is decreased for all the harmonic orders, whereas, for bus T1, it gets decreased only for the harmonic orders 3rd, 5th and the 13th.

The harmonic current flow in the different components as well as in the STATCOM is shown in Fig. 11. The harmonic current drawn from the grid is higher than that in the base case, when the compensation is provided at bus T1. By Kirchhoff's law, it is obvious that the grid has to supply the current drawn by the WPP as well as the compensating resistance. Thus, the resultant harmonic current in the grid will be the phasor sum of the WPP current and the STATCOM current. When the compensation is provided at bus T2, the grid currents are reduced by over 50% for the 11th harmonic, while there is a smaller reduction for other harmonics, except the 5th harmonic, for which there is an amplification. This amplification is due to the reduction of the total impedance for the 5th harmonic.

B. Time domain simulation

A time domain simulation model has been developed in PSCAD to show the STATCOM controller emulating the resistive behavior. The harmonic current source model of the STATCOM is connected to bus T2 as shown in Fig. 4. Its controller measures the T2 bus voltage and extracts the 5th, 7th, 11th, 13th, and the 19th harmonic voltages. Then the corresponding harmonic current references are generated for the emulation of 1-pu resistance (i.e. 121 Ω) at the selected harmonics.

The harmonic filtering functionality of the STATCOM is activated at 5s. The STATCOM harmonic currents increase slowly due to the presence of double pole at −2 rad/sec for the filtering of the *dq* components. Accordingly, the harmonic components of the voltage decrease at the local bus T2. For the remote bus T1, the 5th and the 13th harmonic orders show attenuation while 7th and the 11th orders get amplified as shown in Table III. The rms value of the selected harmonic compensating currents is 0.0057 pu. Though the numerical values differ from the numbers obtained in the harmonic powerflow program, they exhibit similar trend.

TABLE III. HARMONIC VOLTAGES IN THE BASE CASE AND AFTER COMPENSATION (pu values are shown in percentage to reduce the leading zeros)

H. Order	5th	7th	11th	13th	19th
Bus T1					
Base	0.43%	0.23%	0.47%	0.60%	0.47%
Compensated	0.40%	0.23%	0.52%	0.58%	0.47%
Change	7%	-1%	-11%	2%	0%
Bus T2					
Base	0.34%	0.12%	1.42%	0.25%	0.06%
Compensated	0.29%	0.09%	0.64%	0.21%	0.05%
Change	16%	19%	55%	18%	12%
Current (IF)	0.22%	0.10%	0.44%	0.24%	0.06%

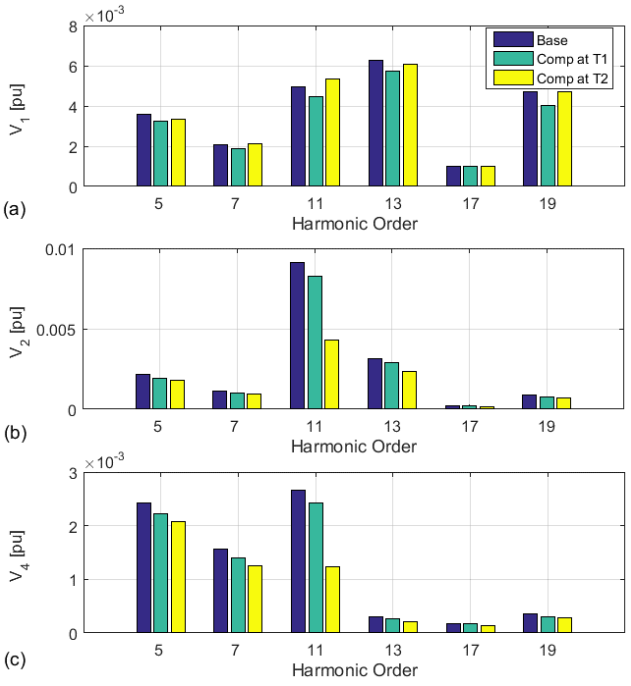

Fig. 10. Harmonic voltages in pu at (a) T1, (b) T2, and (c) T4.

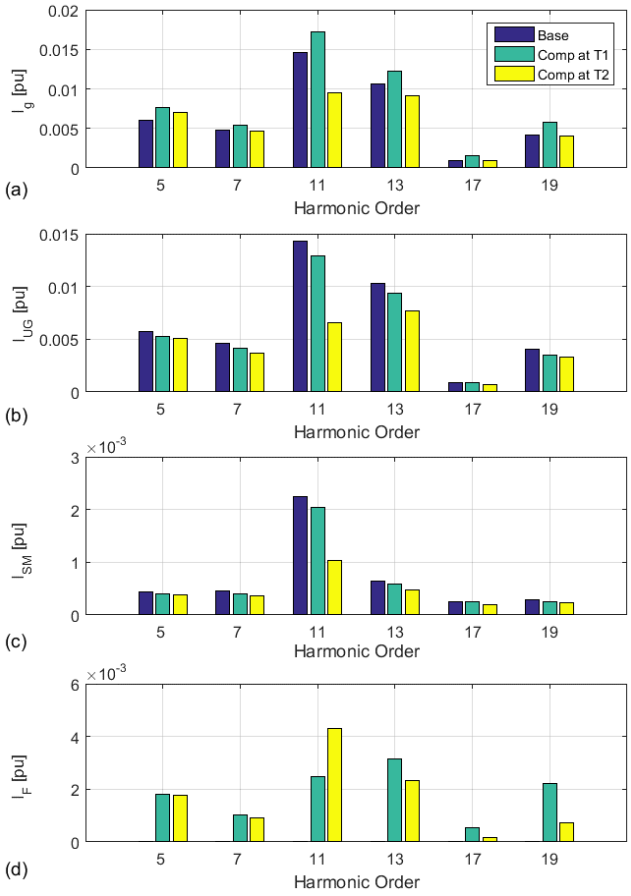

Fig. 11. Harmonic currents in pu. (a) Grid at T1. (b) Underground cable at T2. (c) Sub-marine cable at T4. (d) STATCOM.

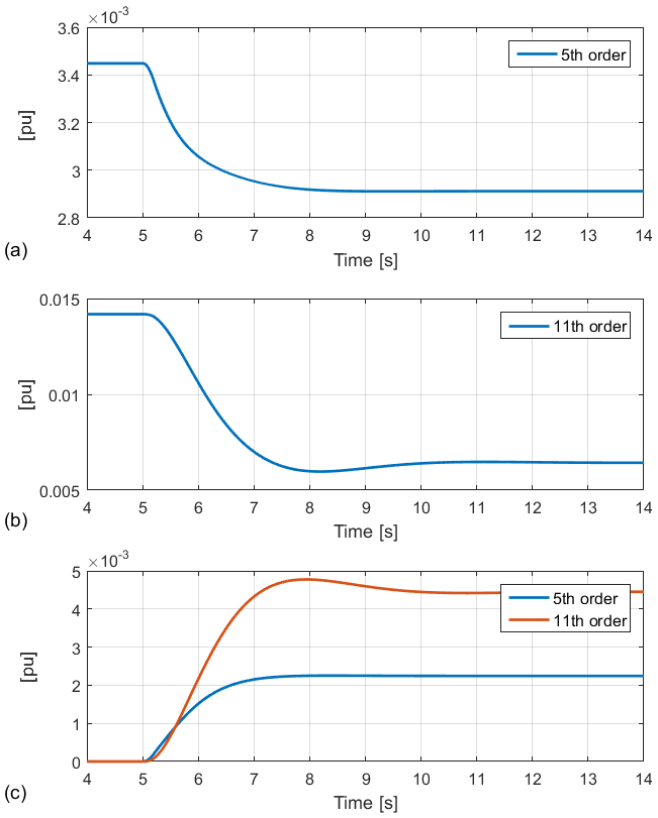

Fig. 12. (a) 5th harmonic voltage at T2. (b) 11th harmonic voltage at T2. (c) 5th and 11th harmonic resistive currents by the STATCOM.

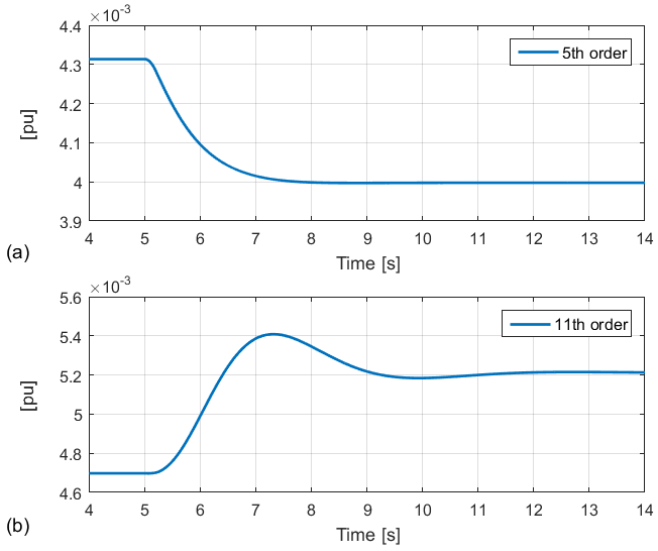

Fig. 13. Harmonic voltages at T1. (a) 5th order. (b) 11th order.

The dynamics of the 5th and 11th order harmonic voltages and the filter currents at T1 and T2 are shown in Fig. 12 and Fig. 13.

V. Conclusion

This work presents the frequency scan of the WPP impedance and analyzes the amplification of the harmonic components of the voltage at two different buses in a test WPP model. The effect of ideal resistive compensation is numerically analyzed and then corroborated using harmonic powerflow analysis. Resistive compensation has the following salient features:

- It is able to attenuate the harmonic voltages at its own bus. Since the WPP has a radial network, the harmonic voltage level gets attenuated downstream from the point of compensation.
- This method does not guarantee attenuation at remote buses upstream from the point of compensation. Rather, in some cases, there might be an amplification of harmonics. In the test system, the 5th and 13th orders were attenuated while there was an amplification for the 7th and 11th orders. Therefore, all different scenarios should be evaluated to ensure that there is no undue amplification at the PCC and other buses upstream.

The resistive compensation is realized using a STATCOM, which emulates the resistive behavior for the selected harmonic orders. Since the STATCOM controller determines the harmonic current references, its effective resistance can be adapted dynamically in real time.

References

[1] M. Bradt et al., "Harmonics and resonance issues in wind powerplants," in IEEE PES GM, San Diego, CA, 2011.

[2] IEEE Std. 519-1992, "IEEE Recommended Practices and Requirements for Harmonic Control in Electrical Power Systems".

[3] IEC Standard 61000-3-6 (2008), Electromagnetic compatibility (EMC) – Part 3-6 – Limits: Assessment of the connection of the distorting installation to MV, HV and EHV power systems.

[4] Planning levels for harmonic voltage distortion and connection of non-linear equipment to transmission and distribution networks in the UK, Engineering Recommendations (ER) G5/4-1.

[5] Gustavsen and H. M. J. De Silva, "Inclusion of rational models in an electromagnetic transients program: Y-Parameters, Z-Parameters, S-parameters, transfer functions," *IEEE Trans. Power Deliv.*, vol. 28, no. 2, pp. 1164–1174, 2013.

[6] Ł. H. Kocewiak *et al.*, "Active Filtering Application in Large Offshore Wind Farms," in International Workshop on Large-Scale Integration of Wind Power into Power Systems as well as Transmission Networks for Offshore Wind Farms, Berlin, 2014.

[7] H. Akagi, H. Fujita, and K. Wada, "A shunt active filter based on voltage detection for harmonic termination of a radial power distribution line," *IEEE Trans. Ind. Appl.*, vol. 35, no. 3, pp. 638–645, 1999.

[8] B. Badrzadeh *et al.*, "Power system harmonic analysis in wind power plants — Part I: Study methodology and techniques," Industry Applications Society Annual Meeting (IAS), 2012 IEEE, Las Vegas, NV, 2012.